International Journal of
Molecular Sciences

MDPI

Article

Effect of $ZnSO_4$, $MnSO_4$ and $FeSO_4$ on the Partial Hydrogenation of Benzene over Nano Ru-Based Catalysts

Haijie Sun [1], Yiru Fan [1], Xiangrong Sun [1], Zhihao Chen [2,*], Huiji Li [1], Zhikun Peng [3,*] and Zhongyi Liu [3]

[1] School of Chemistry and Chemical Engineering, Zhengzhou Normal University, Zhengzhou 450044, China; sunhaijie406@zznu.edu.cn (H.S.); FyR158905@sohu.com (Y.F.); sun1398041920@sohu.com (X.S.); huijili@zznu.edu.cn (H.L.)
[2] Zhengzhou Tobacco Research Institute of CNTC, Zhengzhou 450001, China
[3] College of chemistry and molecular engineering, Zhengzhou University, Zhengzhou 450001, China; liuzhongyi406@sohu.com
* Correspondence: chenzh@ztri.com.cn (Z.C.); pengzhikun@zzu.edu.cn (Z.P.); Tel.: +86-371-6767-2762 (Z.C.)

Abstract: Nano Ru-based catalysts, including monometallic Ru and Ru-Zn nanoparticles, were synthesized via a precipitation method. The prepared catalysts were evaluated on partial hydrogenation of benzene towards cyclohexene generation, during which the effect of reaction modifiers, i.e., $ZnSO_4$, $MnSO_4$, and $FeSO_4$, was investigated. The fresh and the spent catalysts were thoroughly characterized by XRD, TEM, SEM, XPS, XRF, and DFT studies. It was found that Zn^{2+} or Fe^{2+} could be adsorbed on the surface of a monometallic Ru catalyst, where a stabilized complex could be formed between the cations and the cyclohexene. This led to an enhancement of catalytic selectivity towards cyclohexene. Furthermore, electron transfer was observed from Zn^{2+} or Fe^{2+} to Ru, hindering the catalytic activity towards benzene hydrogenation. In comparison, very few Mn^{2+} cations were adsorbed on the Ru surface, for which no cyclohexene could be detected. On the other hand, for Ru-Zn catalyst, Zn existed as rodlike ZnO. The added ZnSO4 and $FeSO_4$ could react with ZnO to generate $(Zn(OH)_2)_5(ZnSO_4)(H_2O)$ and basic Fe sulfate, respectively. This further benefited the adsorption of Zn^{2+} or Fe^{2+}, leading to the decrease of catalytic activity towards benzene conversion and the increase of selectivity towards cyclohexene synthesis. When 0.57 mol·L^{-1} of $ZnSO_4$ was applied, the highest cyclohexene yield of 62.6% was achieved. When $MnSO_4$ was used as a reaction modifier, H_2SO_4 could be generated in the slurry via its hydrolysis, which reacted with ZnO to form $ZnSO_4$. The selectivity towards cyclohexene formation was then improved by the adsorbed Zn^{2+}.

Keywords: benzene; partial hydrogenation; cyclohexene; reaction modifier; $ZnSO_4$; $MnSO_4$; $FeSO_4$

Citation: Sun, H.; Fan, Y.; Sun, X.; Chen, Z.; Li, H.; Peng, Z.; Liu, Z. Effect of $ZnSO_4$, $MnSO_4$ and $FeSO_4$ on the Partial Hydrogenation of Benzene over Nano Ru-Based Catalysts. *Int. J. Mol. Sci.* **2021**, *22*, 7756. https://doi.org/10.3390/ijms22147756

Academic Editor: Raghvendra Singh Yadav

Received: 30 June 2021
Accepted: 16 July 2021
Published: 20 July 2021

1. Introduction

Cyclohexene, a compound with an unstable double bond, can be utilized to synthesize adipic acid, cyclohexanol, and cyclohexanone [1], which are important monomers for the production of nylon 6 and nylon 66. Dehydration of cyclohexanol, dehydrochlorination of halogenated cyclohexane, and Birch reduction methods were traditionally applied for the production of cyclohexene. However, high cost of crude material, side products, and environmental issues are generally addressed, limiting the industrialization of cyclohexene production [2]. In comparison, because of safety, energy conservation, environmental friendliness, and high carbon atom economy, great attention is drawn to the production of cyclohexene via partial hydrogenation of benzene, of which the reaction mechanism is given in Scheme 1. As can been seen in Scheme 1, cyclohexane formation could be done either by direct hydrogenation of benzene or via cyclohexene as an intermediate. It was also reported by Rochin et al. [3] that 1,3-cyclohexadiene could not be detected since diene is extremely unstable due to the further hydrogenation. On the other hand, unfortunately, it is thermodynamically difficult to obtain cyclohexene, since the standard free energy change for cyclohexane formation from benzene hydrogenation is −98 kJ mol^{-1}, which is

much lower than that for selective hydrogenation to cyclohexene, i.e., −23 kJ mol^{-1} [4]. Therefore, it is of great necessity to develop a suitable catalytic system with high selectivity towards cyclohexene generation.

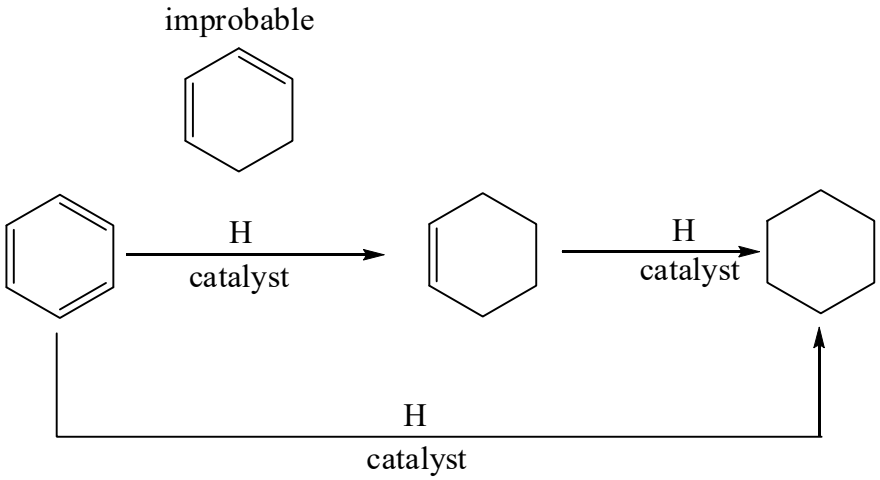

Scheme 1. Reaction mechanism for hydrogenation of benzene.

A reaction modifier is one of the most effective approaches to improve the selectivity towards cyclohexene [5–7] by adding one or several compounds into the reaction slurry to modify the surface of catalysts. In general, cyclohexene can hardly be obtained without applying any reaction modifiers over Ru catalysts [8]. $ZnSO_4$, $FeSO_4$, $CdSO_4$, $CoSO_4$, $NiSO_4$, $CuSO_4$, and $MgSO_4$ were reported as reaction modifiers for partial hydrogenation of benzene towards cyclohexene formation over Ru-based catalysts, among which $ZnSO_4$ and $FeSO_4$ were considered the most effective ones. Notably, it is still controversial in regard to the mechanism for the effect of the reaction modifier. For instance, on one hand, Struijk et al. proposed that the more difficult it is to reduce the cations, the higher are selectivity and yield towards cyclohexene generation [9]. Furthermore, Costa et al. proposed that the oxidation of $ZnNb_2O_6$ contributed to catalytic selectivity over Ru catalysts [10], while Spod et al. stated $Zn(OH)_3^-$ played a significant role in improving the selectivity over Ru catalysts [11]. On the other hand, it was reported by Wang et al. that the binding energy of $Zn2p_{3/2}$ over Ru-Zn/m-ZrO_2 is close to that observed for metallic Zn, declaring that Zn^{2+} was reduced into metallic Zn by the spilled H on the Ru surface [12]. Interestingly, both metallic Zn and Zn^{2+} were observed over Ru-Zn/HAP by Zhang et al. [13]. In general, the effect of Zn can be addressed as follows: (1) the bonding status of hydrogen on the catalyst surface was modified by Zn [14]. The total amount of bonded hydrogen was declined, while the amount of weak bonded hydrogen was enhanced, leading to lower activity towards benzene conversion and higher selectivity towards cyclohexene, respectively; (2) Zn could cover part of the active sites, which is favorable for complete hydrogenation of benzene towards cyclohexane generation [12]; (3) some electrons could be transferred from Zn to Ru, and $Ru^{\delta-}$ might benefit the formation of cyclohexene [12,13]; (4) the adsorption of cyclohexene on the Ru surface could be retarded by the presence of Zn, hindering the further hydrogenation of cyclohexene to cyclohexane [15]. Generally, these controversies are mainly attributed to the development of technologies for the catalyst characterization. Therefore, for the better design of the Ru-based catalytic system on partial hydrogenation of benzene towards cyclohexene production, it is of great significance to reveal the state of Zn and the effect of reaction additives.

Based on the aforementioned situation, $ZnSO_4$, $FeSO_4$, and $MnSO_4$ were applied for the partial hydrogenation of benzene towards cyclohexene formation over monometallic Ru catalyst and Ru-Zn catalyst. The mechanism in which the reaction modifier affects the catalytic activity of nano Ru-based catalysts was thoroughly investigated by XRD, XRF, TEM, and XPS.

2. Results and Discussions

2.1. Ru Catalyst

Figure 1 illustrates the XRD patterns of the monometallic Ru catalyst after the catalytic experiments applying different amount of $ZnSO_4$, $FeSO_4$, and $MnSO_4$ as reaction modifiers. As can be observed, characteristic diffractions corresponding to metallic Ru were shown over all measured samples, demonstrating that Ru existed mainly as the metallic state during the hydrogenation reaction. Furthermore, the particle size of the monometallic Ru catalyst before and after catalytic experiments was calculated via the Scherrer equation and is listed in Table 1. In comparison to the fresh sample, no obvious change was observed for Ru particle size after the hydrogenation reaction with different amounts of $ZnSO_4$, $FeSO_4$, and $MnSO_4$ as reaction modifiers. The particle size of all samples ranged from 3.5 nm to 3.7 nm, which was extremely comparable to that of fresh Ru nanoparticle. This suggests that the particle size of Ru was not affected by the utilization of a reaction modifier.

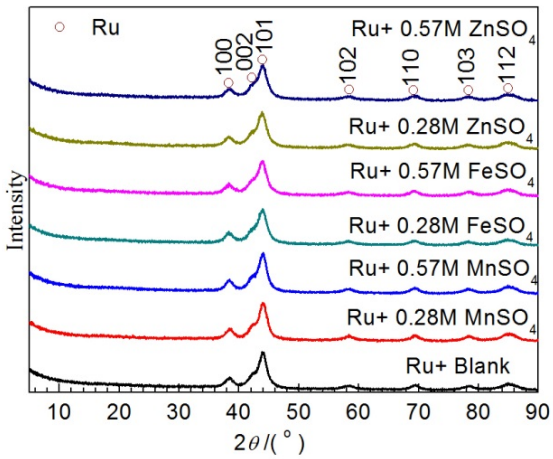

Figure 1. XRD patterns of the monometallic Ru catalyst after catalytic experiments applying different amounts of $ZnSO_4$, $FeSO_4$, and $MnSO_4$ as reaction modifiers.

Table 1. Composition and particle size of the monometallic Ru before and after catalytic experiments with different amounts of reaction modifiers as well as the pH value of slurry.

Conditions	*n*(Zn)/*n*(Ru) [1] (mol/mol)	*n*(Mn)/*n*(Ru) [1] (mol/mol)	*n*(Fe)/*n*(Ru) [1] (mol/mol)	Particle Size [2] (nm)	pH Value [3]
Ru catalyst	-	-	-	3.6	-
Ru + Blank	-	-	-	3.6	6.95
Ru + 0.28 M $MnSO_4$	-	0.0019	-	3.7	3.23
Ru + 0.57 M $MnSO_4$	-	0.0023	-	3.6	3.11
Ru + 0.28 M $FeSO_4$	-	-	0.0358	3.5	4.66
Ru + 0.57 M $FeSO_4$	-	-	0.0295	3.7	3.83
Ru + 0.28 M $ZnSO_4$	0.0307	-	-	3.6	4.35
Ru + 0.57 M $ZnSO_4$	0.0258	-	-	3.7	3.53

[1] Determined by XRF instrument; [2] determined by XRD instrument; [3] pH value of the slurry after catalytic experiments at room temperature.

Table 1 gives the composition of the Ru catalyst before and after catalytic experiments as well as the pH value of the slurry. As observed, only Ru was detected over the fresh Ru catalyst and Ru after hydrogenation reaction in pure distilled water. In comparison, Zn, Fe, and Mn were observed when 0.28 mol L^{-1} of $ZnSO_4$, $FeSO_4$, and $MnSO_4$ were applied as reaction modifiers, respectively. Moreover, the molar ratio of added metal to Ru ranged from Fe > Zn > Mn, implying that the ability of adsorption on the Ru surface ranged from $FeSO_4$ > $ZnSO_4$ > $MnSO_4$. Additionally, the pH value of slurry after the catalytic experiments ranged from the same order, demonstrating that $MnSO_4$ provided the most acidic condition through its hydrolysis. This suggests that the more easily the salt was hydrolyzed, the more difficult it was to adsorb on the Ru surface. Interestingly, when the

concentration of applied reaction modifier was increased to 0.57 mol L^{-1}, the amount of adsorbed metal was decreased. This can be rationalized considering that, by enhancing the concentration of the added modifier, the slurry became more acidic due to the hydrolysis of the metal salts, for which the adsorption of the corresponding metal was retarded. This was also confirmed by the pH value of the slurry after the hydrogenation reaction.

Figure 2 demonstrates the TEM images of the fresh Ru nanoparticles (Figure 2a) and the SEM image as well as the element mapping image of the Ru catalyst after catalytic experiments adding 0.57 mol L^{-1} of $ZnSO_4$, $FeSO_4$, and $MnSO_4$ (Figure 2b–d). As can be seen from Figure 2a, the fresh monometallic Ru catalyst displayed a circular or an elliptical shape. The particle size of Ru was around 3.5 nm, which was in good agreement with XRD results. In addition, it was shown from Figure 2b,c that plenty of Zn and Fe were adsorbed on the Ru surface. On the contrary, only a few Mn were observed from Figure 2c. This was consistent with XRF results (i.e., n(Mn)/n(Ru) was only 0.0023).

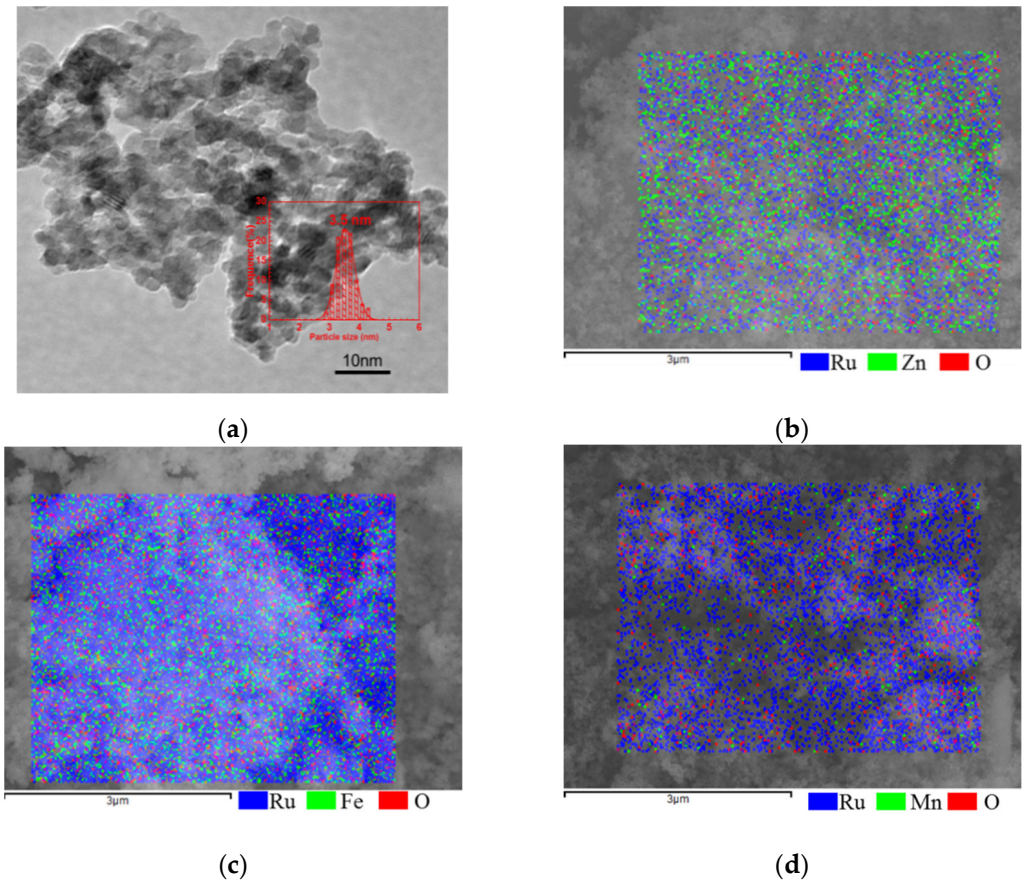

Figure 2. TEM images (**a**) as well as particle size distribution of the fresh Ru nanoparticles (insert image) and the SEM image as well as the element mapping image of Ru catalyst after catalytic experiments adding 0.57 mol L^{-1} of $ZnSO_4$ (**b**), $FeSO_4$ (**c**), and $MnSO_4$ (**d**).

Figure 3 shows the XPS spectra of the monometallic Ru catalyst after hydrogenation reaction applying 0.57 mol L^{-1} of $ZnSO_4$, $FeSO_4$, and $MnSO_4$ as the reaction modifiers, respectively. As can be observed from Figure 3a, two peaks related to binding energies (BE) of 709.8 eV and 712.2 eV were attributed to Fe^{2+} and Fe^{3+}, respectively. The peak at 719.3 eV was related to Fe^{3+} [16]. Furthermore, the peak area of Fe^{2+} was significantly larger than that of Fe^{3+}, indicating that the adsorbed Fe mainly existed as Fe^{2+}. From Figure 3b,c, the BE of Zn $2p_{3/2}$ and Zn LMM was shown at 1021.5 eV and 988.9 eV, respectively. The BE was the same as Zn^{2+}, which was reported by Sun et al. [17–19], suggesting that the adsorbed Zn mainly existed as Zn^{2+}. Unfortunately, due to the extremely low amount of adsorbed Mn, no reflection attributed to Mn^{2+} was observed. As illustrated in Figure 3d, the BE of

Ru $3d_{5/2}$ was 280.1 eV when no reaction modifier was added, which belonged to metallic Ru. This further proved Ru existed mainly as the metallic state during the hydrogenation reaction. Applying $MnSO_4$ as a reaction modifier, the BE of Ru $3d_{5/2}$ was still observed at 280.1 eV, implying that no electron transfer occurred between Ru and Mn. On the other hand, when $ZnSO_4$ and $FeSO_4$ were used, the BE of Ru $3d_{5/2}$ increased from 280.1 eV to 280.6 eV and 280.9 eV, respectively. This can be rationalized by the fact that some electrons were transferred from Ru to Zn and Fe, generating $Ru^{\delta+}$. In addition, it was deemed that more electrons were transferred from Ru to Fe than from Ru to Zn.

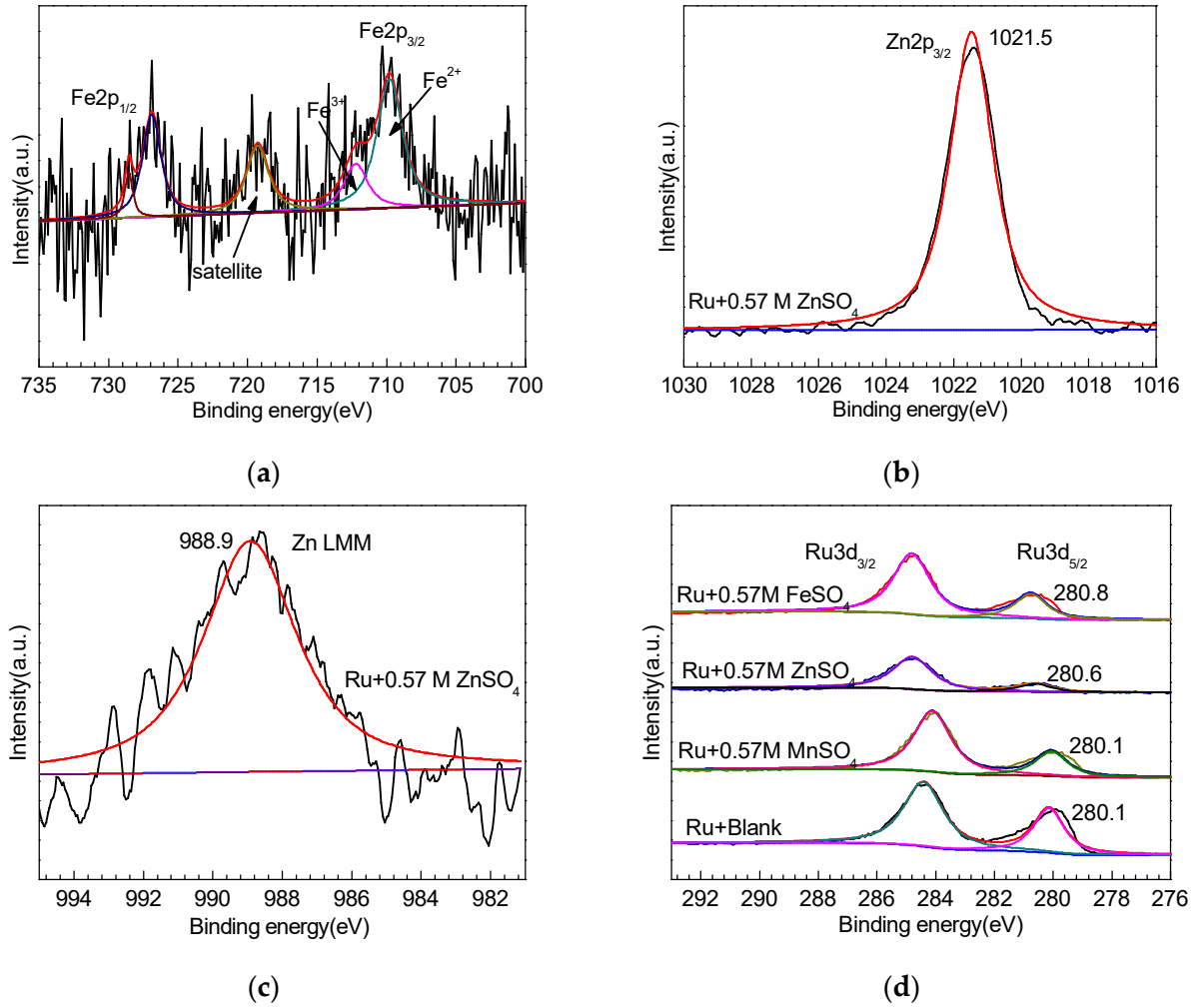

Figure 3. XPS profiles of the monometallic Ru catalyst after hydrogenation reaction applying 0.57 mol L^{-1} of $ZnSO_4$, $FeSO_4$, and $MnSO_4$ as the reaction modifiers. (**a**) Fe 2p over the monometallic Ru catalyst applying 0.57 mol L^{-1} $FeSO_4$; (**b**) Zn $2p_{3/2}$ over the monometallic Ru catalyst applying 0.57 mol L^{-1} $ZnSO_4$; (**c**) Zn LMM over the monometallic Ru catalyst applying 0.57 mol L^{-1} $ZnSO_4$, and (**d**) Ru 3d applying 0.57 mol L^{-1} of $ZnSO_4$, $FeSO_4$, and $MnSO_4$ as the reaction modifiers.

The privileged structure of the formed complex between single/double cyclohexene molecules and cations is shown in Figure 4, and the corresponding Gibbs free energy ($\Delta_f G$) is given in Table 2. As can be seen, the $\Delta_f G$ of the formed complex between Mn^{2+} and a single cyclohexene molecule was −1723 kJ mol^{-1}, and lower $\Delta_f G$ of −1794 kJ mol^{-1} was observed over the complex formed by Fe^{2+} and a single cyclohexene molecule. The most negative $\Delta_f G$ of −1866 kJ mol^{-1} was obtained over the complex formed between Zn^{2+} and a single cyclohexene molecule. Furthermore, the same trend of $\Delta_f G$ was noticed over the formed complex between two cyclohexene molecules and the cations. This showed that Zn^{2+} was the most suitable cation to stabilize cyclohexene by forming a complex.

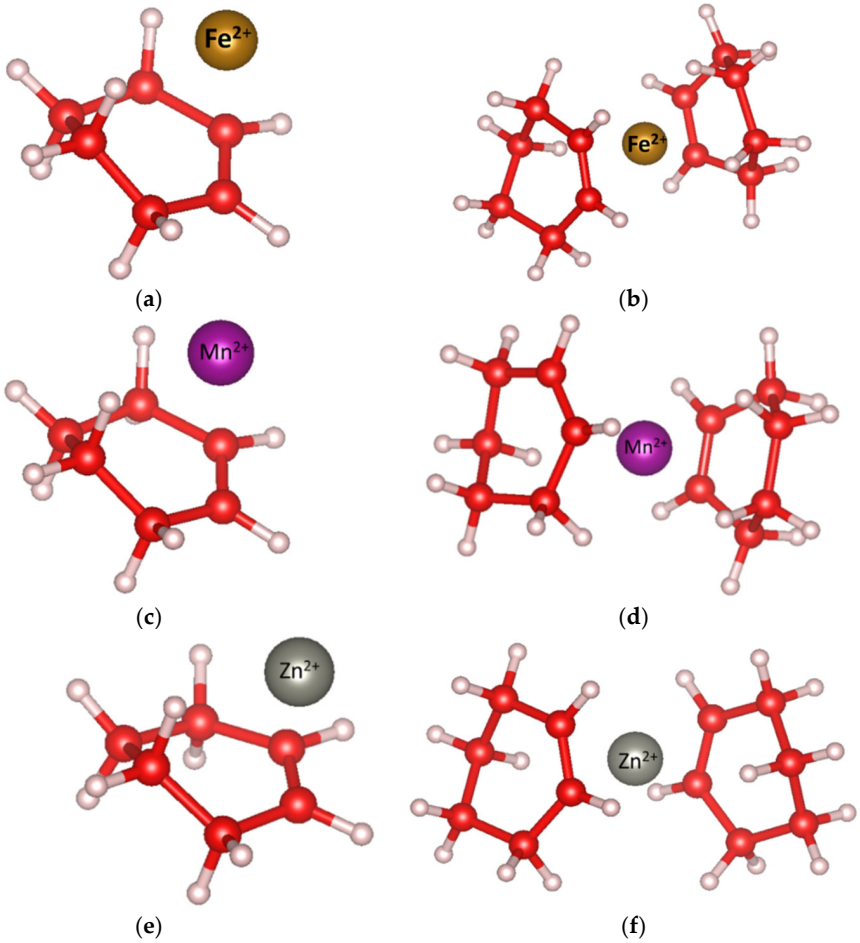

Figure 4. The privileged structure of the formed complex between single/double cyclohexene molecule and Fe^{2+}, Mn^{2+}, as well as Zn^{2+}. (**a**) Fe^{2+} and single cyclohexene molecule; (**b**) Fe^{2+} and double cyclohexene molecules; (**c**) Mn^{2+} and single cyclohexene molecule; (**d**) Mn^{2+} and double cyclohexene molecules; (**e**) Zn^{2+} and single cyclohexene molecule; and (**f**) Zn^{2+} and double cyclohexene molecules.

Table 2. The Gibbs free energy of the formed complex between single/double cyclohexene molecules and cations.

Complex	$\Delta_f G$/(kJ·mol^{-1})
Cyclohexene Mn(II)	−1723
(Cyclohexene)$_2$Mn(II)	−1598
Cyclohexene Fe(II)	−1794
(Cyclohexene)$_2$Fe(II)	−1661
Cyclohexene Zn(II)	−1866
(Cyclohexene)$_2$Zn(II)	−1815

Catalytic activity towards benzene conversion and cyclohexene selectivity over monometallic Ru catalyst with different reaction modifiers are illustrated in Figure 5. Notably, complete conversion of benzene was observed within 5 min when $MnSO_4$ (both 0.28 and 0.57 mol L^{-1}) was applied, and no cyclohexene was detected. Similar results were obtained when no reaction modifier was added, where 100% of benzene was converted to cyclohexane within 5 min of reaction time. In comparison, when $ZnSO_4$ or $FeSO_4$ were used, catalytic activity towards benzene conversion over monometallic Ru was retarded, while cyclohexene selectivity was increased. With increasing the concentration of used reaction modifier (e.g., $ZnSO_4$ or $FeSO_4$), catalytic activity towards benzene conversion was enhanced and selectivity to cyclohexene dropped. In addition, higher benzene conversion

and lower cyclohexene selectivity was observed with applying $ZnSO_4$ than that obtained with utilizing $FeSO_4$ as the reaction modifier. Based on the characterization results, it is deemed that the effect of reaction modifier is mainly attributed to the adsorption of cation. When $MnSO_4$ is added, Mn^{2+} was barely adsorbed on the Ru surface, thus the catalytic activity and selectivity towards cyclohexene formation was not influenced. Additionally, the amount of adsorbed Zn^{2+} or Fe^{2+} was declined with raising the concentration of applied $ZnSO_4$ or $FeSO_4$, respectively. This leads to the higher catalytic activity towards benzene conversion and lower selectivity towards cyclohexene generation. How the adsorbed Zn^{2+} and Fe^{2+} affecting the partial hydrogenation of benzene over Ru catalysts can be addressed as following: 1. some electrons could be transferred from Ru to Zn^{2+}/Fe^{2+} to generate $Ru^{\delta+}$, which is less active for activation the π orbital of benzene. Only two of the π orbital of benzene was activated, resulting in the synthesis of cyclohexene via a partial hydrogenation procedure [20]; 2. more stabilized complex could be formed between Zn^{2+}/Fe^{2+} and cyclohexene, improving the selectivity towards cyclohexene production [21,22]; 3. the adsorbed Zn^{2+} and Fe^{2+} could cover parts of the active sites of Ru for H_2 dissociation, hence benefiting the cyclohexene formation [9]. Thus, with increasing the concentration of $ZnSO_4/FeSO_4$, the amount of adsorbed Zn^{2+}/Fe^{2+} was declined, hence the selectivity towards cyclohexene was decreased. Furthermore, more Fe^{2+} was adsorbed on the Ru surface than that observed for Zn^{2+}, leading to more electron transfer and more active sites coverage for Fe than that for Zn. It is therefore lower catalytic activity towards benzene conversion and higher cyclohexene selectivity was achieved over monometallic Ru catalyst with applying $FeSO_4$ than using $ZnSO_4$.

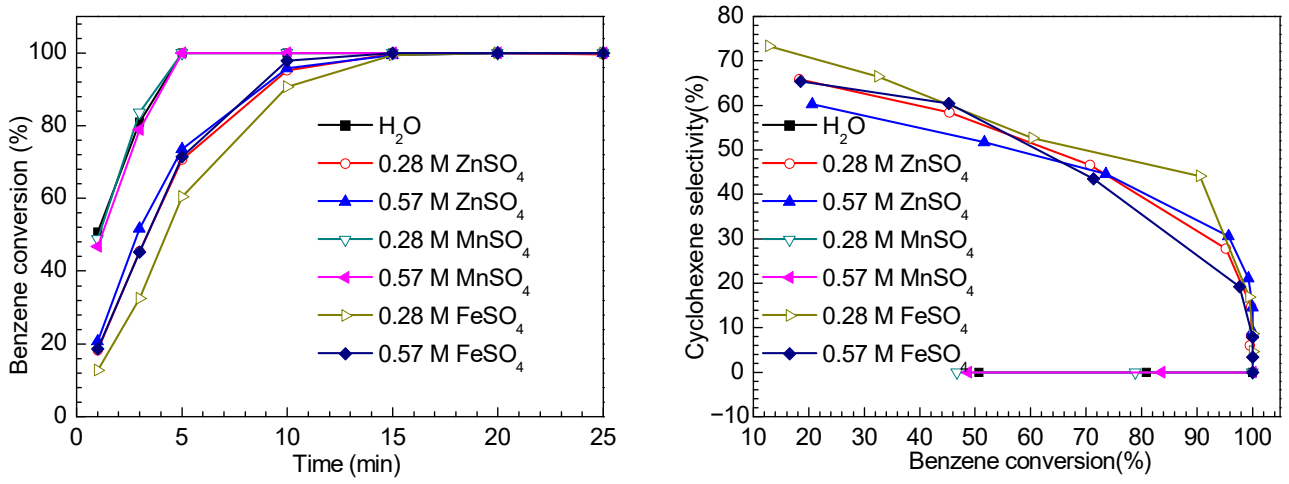

Figure 5. Catalytic activity towards benzene conversion and cyclohexene selectivity over the monometallic Ru catalyst with different reaction modifiers (m_{cat} = 1.8 g, V_{H2O} = 280 mL, $V_{benzene}$ = 140 mL, T = 423 K, p H_2 = 5.0 MPa) (**a**): benzene conversion; (**b**): cyclohexene selectivity.

2.2. Ru-Zn Catalyst

Figure 6 exhibits the XRD patterns of the Ru-Zn catalyst after catalytic experiments applying different amounts of $ZnSO_4$, $FeSO_4$, and $MnSO_4$ as reaction modifiers. As can be observed, characteristic diffractions corresponding to metallic Ru with the hexagonal phase and ZnO with the hexagonal phase were observed over Ru-Zn after hydrogenation without adding any reaction modifier, demonstrating that Ru and Zn existed mainly as metallic Ru and ZnO, respectively. Applying $MnSO_4$ or $FeSO_4$ (both 0.28 and 0.57 mol L^{-1}), the reflection to ZnO could no longer be observed. This can be attributed to the fact that $MnSO_4$ or $FeSO_4$ could react with ZnO to form new compounds, which were dissolvable under the reaction conditions. When $ZnSO_4$ was added as a reaction modifier, a new diffraction related to $(Zn(OH)_2)_5(ZnSO_4)(H_2O)$ was observed, indicating that ZnO could

react with $ZnSO_4$ to generate $(Zn(OH)_2)_5(ZnSO_4)(H_2O)$. The same results were reported by Sun et al. [23] and Yan et al. [24].

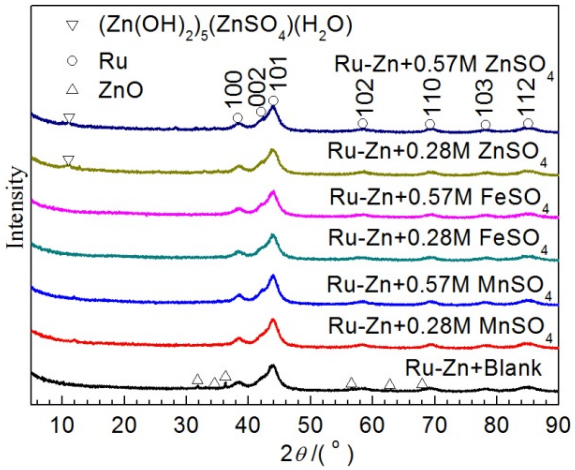

Figure 6. XRD patterns of the Ru-Zn catalyst after catalytic experiments applying different amounts of $ZnSO_4$, $FeSO_4$, and $MnSO_4$ as reaction modifiers.

Table 3 lists the composition and the particle size of the Ru-Zn catalyst after catalytic experiments as well as the pH value of the slurry. Without using any reaction modifier, the molar ratio of Zn to Ru was close to that of the fresh Ru-Zn catalyst (e.g., n(Zn)/n(Ru) = 0.2645), suggesting that Zn was barely lost during the catalytic experiment. The slurry was close to neutral (pH = 6.95). When 0.28 mol L^{-1} of $MnSO_4$ was used, n(Zn)/n(Ru) was decreased from 0.2645 to 0.2228, and n(Mn)/n(Ru) was also raised in comparison to that observed over the monometallic Ru catalyst (e.g., 0.0247 vs. 0.0019). This was mainly because the acidic condition was neutralized by ZnO. Hence, the pH value of the slurry increased, resulting in more Mn^{2+} and SO_4^{2-} being adsorbed on the Ru surface. While the concentration of used $MnSO_4$ was increased to 0.57 mol L^{-1}, the slurry became more acidic, leading to less adsorption of Zn^{2+}, Mn^{2+}, and SO_4^{2-} than that obtained with 0.28 mol L^{-1} of $MnSO_4$. Furthermore, with addition of 0.28 mol L^{-1} of $ZnSO_4$, the n(Zn)/n(Ru) slightly dropped in comparison to that detected without any reaction modifier (e.g., 0.2360 vs. 0.2645). This can be rationalized considering that part of ZnO was dissolved under such acidic conditions. However, a significant increase of S was observed, i.e., n(S)/n(Ru) = 0.0216, and the molar ratio of Zn to Ru was obviously higher than that observed over the monometallic Ru catalyst under the same conditions (e.g., 0.2360 vs. 0.0307). This was mainly due to the formation of $(Zn(OH)_2)_5(ZnSO_4)(H_2O)$ salt from the reaction between ZnO and $ZnSO_4$, which benefited the adsorption of Zn^{2+}. By enhancing the concentration of $ZnSO_4$ from 0.28 mol L^{-1} to 0.57 mol L^{-1}, the pH value decreased from 6.08 to 5.61. This resulted in the lower content of formed $(Zn(OH)_2)_5(ZnSO_4)(H_2O)$, hence the adsorbed Zn^{2+}. On the other hand, when $FeSO_4$ was applied, a severe decline of adsorbed Zn was noticed. It was deemed that $FeSO_4$ could react with ZnO to form salt-like basic Fe sulfate salt, which depressed the adsorption of Zn. Moreover, the particle size of all Ru-Zn catalysts ranged from 3.7 nm to 3.9 nm after the experiments, suggesting that particle size of Ru-Zn was not affected by the utilization of reaction modifiers.

The TEM and the SEM images as well as the element mapping image of the spent Ru-Zn catalyst without using any reaction modifier are illustrated in Figure 7a,b, respectively. It can be seen from Figure 7a that the spent Ru-Zn catalyst displayed a circular or an elliptical shape, of which particle size was around 3.4 nm. Moreover, rodlike ZnO was observed, indicating that ZnO could not be uniformly dispersed on the surface of the catalyst. As observed from Figure 7b, the rodlike shape of the Zn element was also observed, which was consistent with the TEM results. Figure 7c displays the TEM image of the spent Ru-Zn catalyst applying $ZnSO_4$ (0.57 mol L^{-1}) as the reaction modifier. No

rodlike ZnO was detected, suggesting that ZnO was consumed through the reaction with $ZnSO_4$. Furthermore, the particle size of Ru-Zn was mainly distributed at 3.3 nm, which was comparable to that obtained over spent Ru-Zn without using any reaction modifier. This implied that the particle size of Ru-Zn could not be affected by utilization of the reaction modifier. Figure 7d demonstrates the SEM image as well as the element mapping image of the spent Ru-Zn catalyst using $ZnSO_4$ as a reaction modifier. No rodlike ZnO could be observed, and Zn species was uniformly dispersed on the surface of the Ru-Zn catalyst. This can be rationalized considering that $(Zn(OH)_2)_5(ZnSO_4)(H_2O)$ could be generated and uniformly dispersed on the surface of the Ru-Zn catalyst. When $FeSO_4$ was added (0.57 mol L^{-1}), as shown in Figure 7e, both Zn and Fe species were uniformly dispersed on the surface of the Ru-Zn catalyst. Besides, rodlike ZnO disappeared. A similar phenomenon was observed when $MnSO_4$ (0.57 mol L^{-1}) was applied, where Zn and Mn species were also uniformly dispersed on the surface of the Ru-Zn catalyst. Interestingly, more Mn was observed in comparison to that detected over the monometallic Ru catalyst, indicating an enhancement of adsorbed Mn on the Ru-Zn surface.

Table 3. Composition and particle size of monometallic Ru before and after catalytic experiments with different amounts of reaction modifiers as well as the pH value of slurry.

Conditions	n(Zn)/n(Ru) [1] (mol/mol)	n(Mn)/n(Ru) [1] (mol/mol)	n(Fe)/n(Ru) [1] (mol/mol)	n(S)/n(Ru) (mol/mol)	Particle [2] Size(nm)	pH [3] Value
Ru-Zn(0.27) + Blank	0.2645	-	-	-	3.7	6.95
Ru-Zn(0.27) + 0.28 M $MnSO_4$	0.1528	0.0247	-	0.0078	3.8	6.98
Ru-Zn(0.27) + 0.57 M $MnSO_4$	0.1413	0.0225	-	0.0053	3.9	6.85
Ru-Zn(0.27) + 0.28 M $FeSO_4$	0.0624	-	0.2422	0.0032	3.7	6.92
Ru-Zn(0.27) + 0.57 M $FeSO_4$	0.0542	-	0.2782	0.0048	3.8	6.51
Ru-Zn(0.27) + 0.28 M $ZnSO_4$	0.2360	-	-	0.0216	3.8	6.08
Ru-Zn(0.27) + 0.57 M $ZnSO_4$	0.2135	-	-	0.0183	3.9	5.61

[1] Determined by XRF instrument; [2] determined by XRD instrument; [3] pH value of the slurry after catalytic experiments at room temperature.

Figure 8 shows the XPS profiles of the Ru-Zn catalyst after catalytic experiments applying $ZnSO_4$, $FeSO_4$, and $MnSO_4$ (all 0.57 mol L^{-1}) as the reaction modifier, respectively. The BE of Zn $2p_{3/2}$ and Zn LMM over Ru-Zn catalyst using $ZnSO_4$ or $MnSO_4$ as reaction modifier was demonstrated in Figure 8a,b. With addition of $ZnSO_4$, the BEs of Zn $2p_{3/2}$ and Zn LMM over Ru-Zn catalyst were observed at 1021.0 eV and 988.5 eV, respectively. In comparison, when $MnSO_4$ was applied, the BEs of Zn $2p_{3/2}$ and Zn LMM over the Ru-Zn catalyst were observed at 1021.7 eV and 987.1 eV, respectively. It was deemed that Zn mainly existed as Zn^{2+}, as the BE of Zn LMM for metallic Zn was 990.1 eV [25]. More importantly, more electrons were transferred from Zn to Ru using $ZnSO_4$ than those obtained using $MnSO_4$ as the reaction modifier. As can be observed from Figure 8c, two peaks related to binding energies of 710.7 eV and 713.4 eV were attributed to Fe^{2+} and Fe^{3+}, respectively. Besides, the satellite diffraction at 718.6 eV belonged to Fe^{2+} [26]. Furthermore, the peak area of Fe^{2+} was obviously larger than that of Fe^{3+}, suggesting that the adsorbed Fe mainly existed as Fe^{2+}. As observed in Figure 8d, the BE of Mn $2p_{3/2}$ was shown at 644.2 eV, which was attributed to Mn^{2+} [27]. This implied that the adsorbed Mn was not reduced. Furthermore, as illustrated in Figure 8e, the BE of Ru $3d_{5/2}$ was 278.9 eV when no reaction modifier was added, which belonged to metallic Ru. This revealed that undispersed ZnO of Ru-Zn could not affect the electronic structure of Ru. Applying $MnSO_4$ as a reaction modifier, the BE of Ru $3d_{5/2}$ was slightly increased from 278.9 eV to 279.0 eV. Based on the aforementioned discussion, it was already concluded that adsorbed Mn could not affect the electronic structure of Ru. Therefore, combined with the shift for BE of Zn $2p_{3/2}$ and Zn LMM, it was deemed that the slight raise for the BE of Ru $3d_{5/2}$ was attributed to the adsorbed Zn. In addition, an obvious increase of the BE of Ru $3d_{5/2}$ was noticed when $ZnSO_4$ was applied, i.e., from 278.9 eV to 280.2 eV. This can be rationalized in terms of the formation of $(Zn(OH)_2)_5(ZnSO_4)(H_2O)$, which contained more Zn species. Higher amounts of adsorbed Zn resulted in the higher BE of Ru $3d_{5/2}$, implying that more $Ru^{\delta+}$ was generated. Moreover, the highest BE of Ru $3d_{5/2}$ was observed with addition

of $FeSO_4$ (e.g., 280.8 eV), demonstrating that the most electrons were transferred from Ru to Fe.

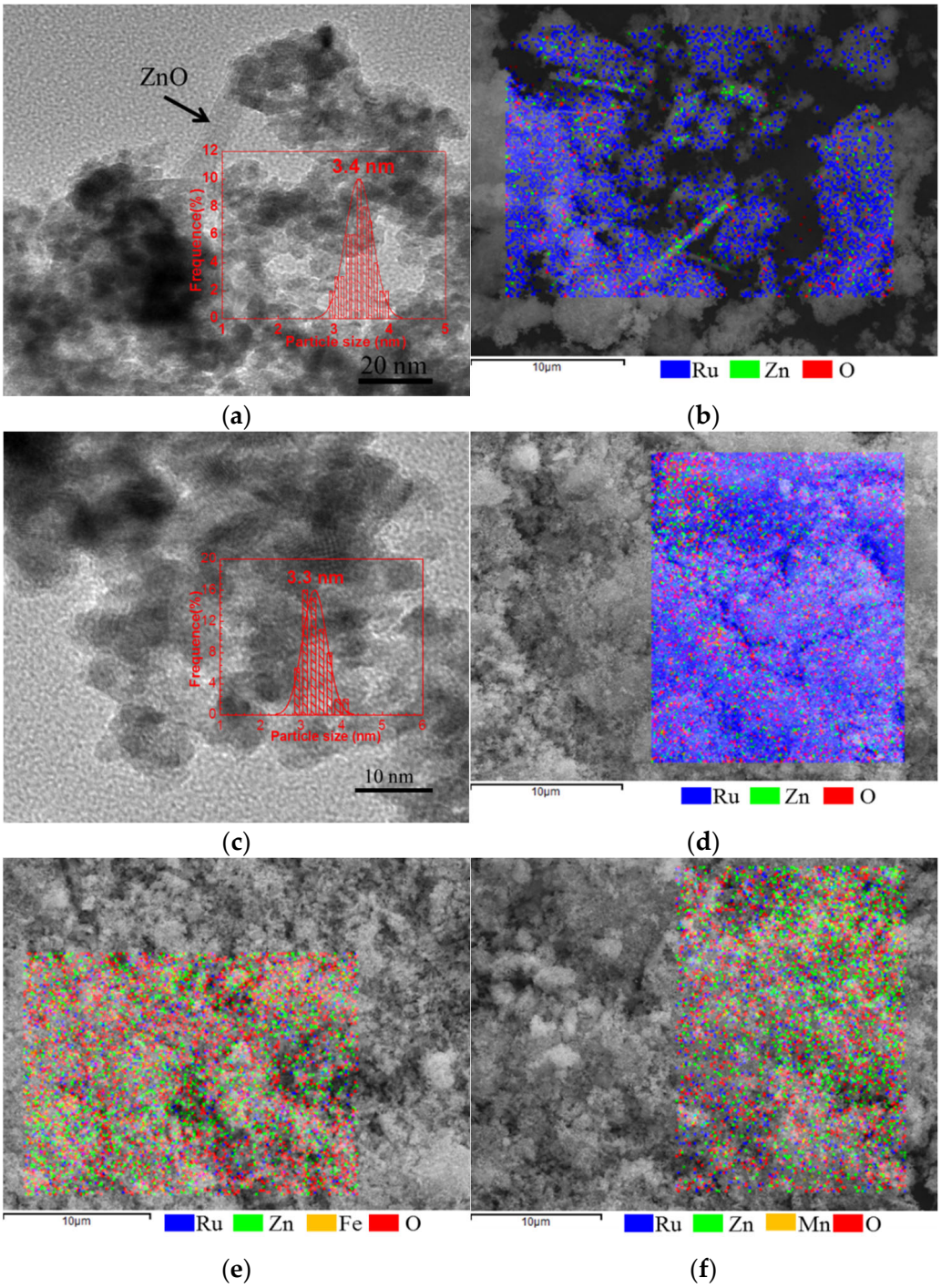

Figure 7. TEM images, SEM images, particle size distribution, and element mapping image of the spent Ru-Zn catalyst with different reaction modifiers added. (**a**) TEM image and particle size distribution (insert image) of the spent Ru-Zn catalyst without using any reaction modifier; (**b**) SEM image as well as element mapping image of the spent Ru-Zn catalyst without using any reaction modifier; (**c**) TEM image of the spent Ru-Zn catalyst applying $ZnSO_4$ (0.57 mol L^{-1}) as the reaction modifier; (**d**) SEM image as well as the element mapping image of the spent Ru-Zn catalyst using $ZnSO_4$ as a reaction modifier; (**e**) SEM image as well as the element mapping image of the spent Ru-Zn catalyst using $FeSO_4$ as a reaction modifier; (**f**) SEM image as well as the element mapping image of the spent Ru-Zn catalyst using $MnSO_4$ as a reaction modifier.

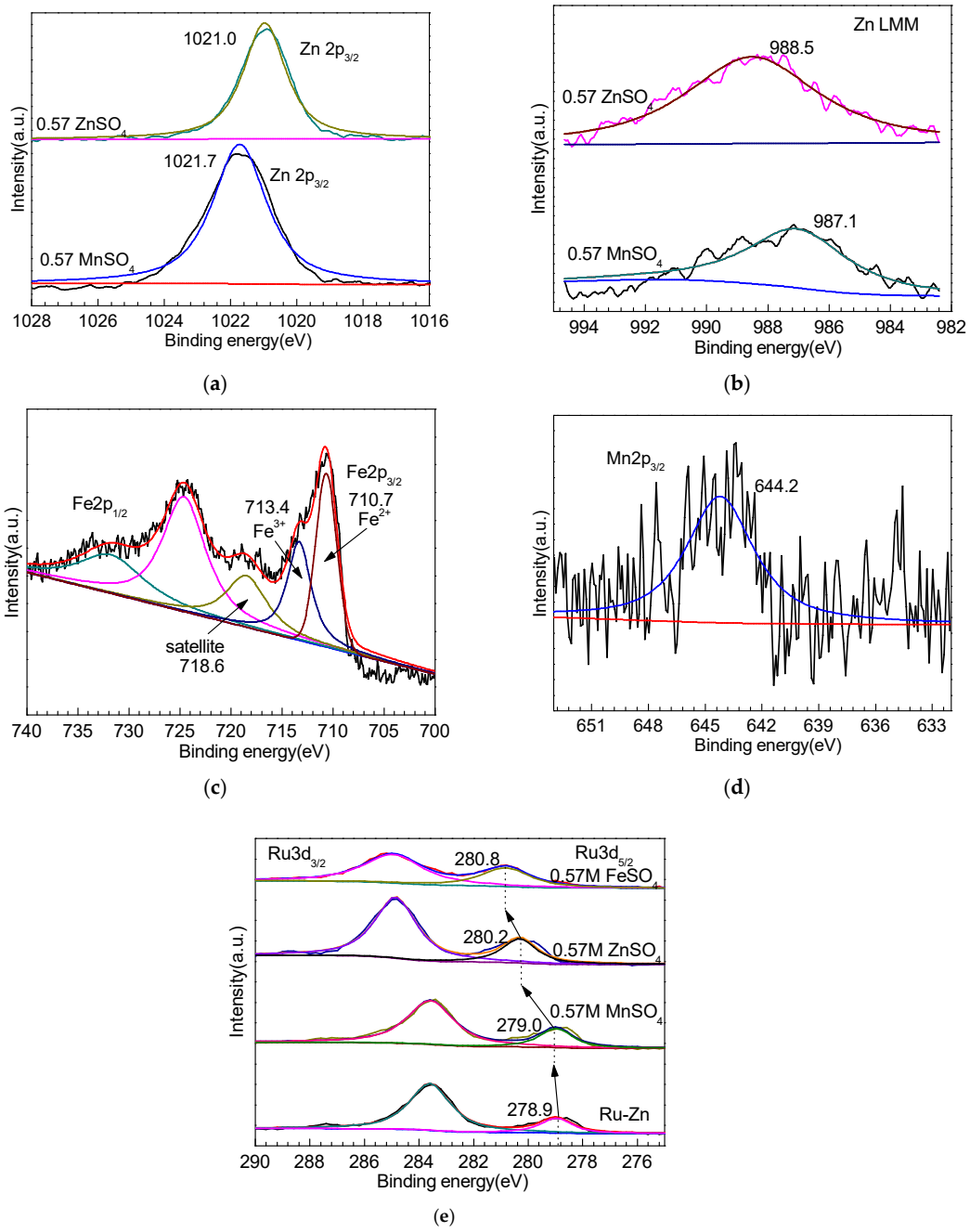

Figure 8. XPS profiles of the Ru-Zn catalyst after hydrogenation reaction applying 0.57 mol L^{-1} of $ZnSO_4$, $FeSO_4$, and $MnSO_4$ as the reaction modifiers. (**a**) Zn $2p_{3/2}$ over the Ru-Zn catalyst applying 0.57 mol L^{-1} of $ZnSO_4$ and $MnSO_4$, respectively; (**b**) Zn LMM over the Ru-Zn catalyst applying 0.57 mol L^{-1} $ZnSO_4$ and $MnSO_4$, respectively; (**c**) Fe 2p over the Ru-Zn catalyst applying 0.57 mol L^{-1} $FeSO_4$; (**d**) Mn $2p_{3/2}$ over the Ru-Zn catalyst applying 0.57 mol L^{-1} $MnSO_4$, and (**e**) Ru $3d_{5/2}$ with and without reaction modifiers.

Catalytic activity towards benzene conversion and cyclohexene selectivity over the Ru-Zn catalyst with different reaction modifiers are illustrated in Figure 9. As can be observed from Figure 9a,b, in comparison to that achieved with no reaction modifier, a significant decrease of catalytic activity towards benzene conversion as well as an increase towards cyclohexene formation were obtained by using reaction modifiers. Among the used reaction modifiers, the lowest benzene conversion and the highest cyclohexene selectivity were achieved over the Ru-Zn catalyst using 0.57 mol L^{-1} of $FeSO_4$, and 0.28 mol L^{-1} of $MnSO_4$ gave the highest benzene conversion and the lowest cyclohexene selectivity within

25 min of reaction time. Notably, a lower concentration of $ZnSO_4$/$MnSO_4$ and a higher concentration of $FeSO_4$ were beneficial for hindering the catalytic activity towards benzene conversion and improving the selectivity towards cyclohexene generation over the Ru-Zn catalyst. Based on the characterization results and discussions, it was deemed that the adsorbed Zn^{2+}/Fe^{2+} played the essential role in the synthesis of cyclohexene from partial hydrogenation of benzene over the Ru-Zn catalyst. This can be rationalized considering that some electrons could be transferred from Ru to Zn^{2+}/Fe^{2+} to generate $Ru^{\delta+}$, which could only activate two of the π orbital of benzene, resulting in benefits for synthesis of cyclohexene via a partial hydrogenation procedure. Furthermore, Zn^{2+}/Fe^{2+} was of great capability to stabilize cyclohexene, for which the further hydrogenation of cyclohexene to cyclohexane was retarded. Additionally, the adsorbed Zn^{2+} and Fe^{2+} could cover parts of the most active sites of Ru for direct hydrogenation of benzene to cyclohexane, thus benefiting the formation of cyclohexene. Considering both catalytic activity towards benzene conversion and selectivity to cyclohexene, $ZnSO_4$ with a concentration of 0.57 mol L^{-1}, among all investigated reaction modifiers, was the most suitable for partial hydrogenation of benzene for cyclohexene production over Ru-Zn catalysts. As observed from Figure 9c,d, 48.1% of cyclohexene yield was achieved over the Ru-Zn catalyst applying 0.57 mol L^{-1} of $ZnSO_4$ as a reaction modifier within 25 min of the catalytic experiment, and the highest cyclohexene yield of 62.6% was obtained when the reaction time reached 40 min, which was one of the highest yields of cyclohexene to ever be reported [4,28].

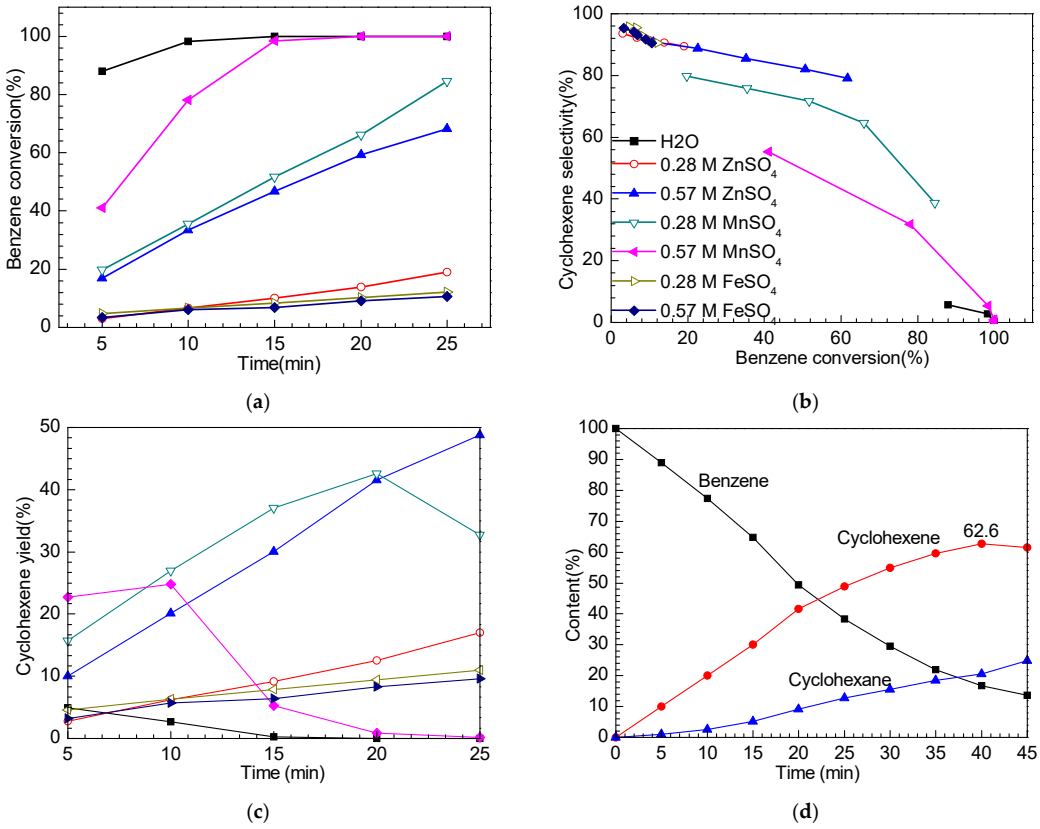

Figure 9. Catalytic activity towards benzene conversion and cyclohexene selectivity over the Ru-Zn catalyst with different reaction modifiers (m_{cat} = 1.8 g, V_{H2O} = 280 mL, $V_{benzene}$ = 140 mL, T = 423 K, p H_2 = 5.0 MPa) (**a**): benzene conversion; (**b**): cyclohexene selectivity; (**c**) cyclohexene yield; and (**d**) kinetic curve over Ru-Zn with addition of 0.57 mol L^{-1} of $ZnSO_4$.

3. Conclusions

Nano Ru-based catalysts, including monometallic Ru and Ru-Zn nanoparticles, were synthesized and evaluated on partial hydrogenation of benzene towards cyclohexene generation, during which the effect of the reaction modifiers, i.e., $ZnSO_4$, $MnSO_4$, and

$FeSO_4$, was investigated. It was found that Zn^{2+} or Fe^{2+} could be adsorbed on the surface of the monometallic Ru catalyst, which could stabilize the formed cyclohexene. This led to an enhancement of catalytic selectivity towards cyclohexene. Furthermore, electron transfer was observed from Zn^{2+} or Fe^{2+} to Ru, hindering the catalytic activity towards benzene conversion. In comparison, very few Mn^{2+} cations were adsorbed on the Ru surface, for which no cyclohexene could be detected. On the other hand, for the Ru-Zn catalyst, Zn existed as rodlike ZnO. The added $ZnSO_4$ and $FeSO_4$ could react with ZnO to generate $(Zn(OH)_2)_5(ZnSO_4)(H_2O)$ and $Fe(OH)SO_4$, respectively. This further benefited the adsorption of Zn^{2+} or Fe^{2+}, leading to the decrease of catalytic activity towards benzene conversion and the increase of selectivity towards cyclohexene synthesis. When 0.57 mol L^{-1} of $ZnSO_4$ was applied, the highest cyclohexene yield of 62.6% was achieved. When $MnSO_4$ was used as a reaction modifier, H_2SO_4 could be generated in the slurry via its hydrolysis, which reacted with ZnO to form $ZnSO_4$. The selectivity towards cyclohexene formation was then improved by the adsorbed Zn^{2+}.

4. Materials and Methods

4.1. Chemicals

All regents were analytical grade. $RuCl_3 \cdot 3H_2O$ was received from Sino-Platinum Co. Ltd. (Kunming, China). NaOH, $FeSO_4 \cdot 7H_2O$, $ZnSO_4 \cdot 7H_2O$, $MnSO_4 \cdot H_2O$, and benzene were purchased from Kemiou Chemical Reagent Co. Ltd. (Tianjin, China). All chemicals were directly used without any further purification, and deionized water was utilized in all experiments.

4.2. Preparation of Catalysts

Ru-Zn catalysts were synthesized via the following procedure: 100 mL of NaOH (0.75 mol·L^{-1}) aqueous solution was added into 100 mL aqueous solution of $RuCl_3$ (0.18 mol·L^{-1}) and $ZnSO_4$ (0.06 mol L^{-1}) with constant stirring at 353 K for 30 min. Then, the solid part was washed until reaching pH = 7. After that, the solid was dispersed in 200 mL of deionized water, followed by a reducing procedure under 5.0 MPa of H_2 in a 1000 mL Hastelloy autoclave with a stirring speed of 800 rpm at 423 K. After 3 h of reduction and cooling to 298 K, the fresh catalysts were gained by washing to neutral and were vacuum-dried. The obtained Ru-Zn catalysts were denoted as Ru-Zn. Similarly, monometallic Ru catalysts were synthesized from the same procedure without introducing $ZnSO_4 \cdot 7H_2O$.

4.3. Catalytic Experimental Procedure

All catalytic experiments took place in a 1000 mL GS-1 type Hastelloy autoclave. In a typical reaction, a Ru-Zn catalyst with 0.57 mol·L^{-1} $ZnSO_4$ as an instance as well as a 1.8 g Ru-Zn catalyst and a 280 mL aqueous solution of 0.57 mol·L^{-1} $ZnSO_4$ were poured into the autoclave. Then, the reactor was purified with N_2 by increasing the pressure to 5 MPa and depressurizing to 0.2 MPa 4 times. This was followed by purification using H_2 another 4 times with the same procedure. Then, the autoclave was heated under 5.0 MPa of H_2 with a stirring speed of 800 rpm. When the temperature reached 423 K, 140 mL of benzene was added into the reactor, and the stirring speed was adjusted to be 1400 rpm to eradicate the effect of mass transfer limitation. Subsequently, the liquid samples were taken from the autoclave every 5 min. All withdrawn samples were analyzed by GC-FID. The benzene conversion and the selectivity towards cyclohexene were calculated with the calibration area normalization method. After each reaction, the catalyst sample was washed until neutral and dried in an Ar atmosphere at 373 K, then stored in ethanol for further characterization. Monometallic Ru and Ru-Zn catalysts with different reaction modifiers were evaluated with the same procedure. In addition, it is important to mention that the mass balance of the reaction was 100% closed.

4.4. Catalysts Characterization

X-ray diffraction (XRD) patterns were obtained at the range of 2θ from 5° to 90°, with a step size of 0.03° using diffracted intensity of Cu-Kα radiation (λ = 0.15418 nm) via an X'Pert Pro instrument (PAN Nallytical, Almelo, The Netherlands). Scherrer's equation was applied for the calculation of the particle size of tested samples. In addition, elemental analysis was conducted via X-ray fluorescence (XRF) (S4 Pioneer instrument from Bruker AXS, Karlsruhe, Germany). Furthermore, the morphology of the catalyst surface as well as the element scanning was tested by transmission electron microscope (TEM), a JEOL JEM 2100 from Akishima, Japan. Surface composition of the selected samples was identified by energy dispersive spectrometer (EDS). Moreover, the valence states of Ru, Zn, Fe, and Mn as well as the kinetic energy of Zn LMM electrons on the catalyst surface were analyzed by X-ray photoelectron spectroscopy (XPS) using a PHI Quantera SXM instrument from ULVAC-PHI, Japan. Al Kα (Eb = 1486.6 eV) was chosen as the radiation source, and the vacuum degree was adjusted to be 6.7×10^{-8} Pa. The C1s (Eb = 284.8 eV) line as the binding energy reference was used for calibrating and correcting the energy scale.

4.5. Theoretical Calculation

The B3LYP density functional method in conjunction with the 6-31G(d,p) basis set for cyclohexene and Lanl2DZ for the metal ions was used to optimize the complexes formed between cyclohexene and the metal ions of Fe^{2+}, Mn^{2+}, and Zn^{2+}. The calculations were all performed with the Gaussian 09 software package. Vibrational frequency analyses were performed for the optimized geometries.

Author Contributions: H.S. and Z.C. were responsible for designing the experiments and the manuscript preparation. Y.F. and X.S. were responsible for conducting the experiments and the data analysis. Z.P. was responsible for making figures. H.L. was responsible for data calculation. Z.L. was responsible for all the chemical purchases and the characterization of the samples. All authors have read and agreed to the published version of the manuscript.

Funding: This research was funded by Key Science and Technology Program of Henan Province, grant number 192102210139; The Training Plan of Young Backbone Teachers in Colleges and Universities of Henan Province, grant number 2019GGJS252; Innovation and Entrepreneurship Training Program for college students in Henan Province, grant number 202112949001; Key Scientific Research Projects of Colleges and Universities in Henan Province, grant number 18A150018; National Natural Science Foundation of China, grant number 21908203; China Postdoctoral Science Foundation, grant number 2019T120637.

Informed Consent Statement: Not applicable.

Data Availability Statement: The data presented in this study are available in this work.

Conflicts of Interest: The authors declare no conflict of interest.

References

1. Pu, J.C.; Dari, M.D.; Tang, X.Q.; Yuan, P.Q. Diffusion of benzene through water film confined in silica mesopores: Effect of competitive adsorption of solvent. *Chem. Eng. Sci.* **2020**, *224*, 115793. [CrossRef]
2. Zhou, G.B.; Jiang, L.; He, D.P. Nanoparticulate Ru on TiO_2 exposed the {100} facets: Support facet effect on selective hydrogenation of benzene to cyclohexene. *J. Catal.* **2019**, *369*, 352–362. [CrossRef]
3. Rochin, L.; Toniolo, L. Selective hydrogenation of benzene to cyclohexene using a suspended Ru catalyst in a mechanically agitated tetraphase reactor. *Catal. Today* **1999**, *48*, 255–264. [CrossRef]
4. Gonçalves, A.H.A.; Soares, J.C.S.; Araújo, L.R.R.; Zotin, F.M.Z.; Mendes, F.M.T.; Gaspar, A.B. Surface investigation by X-ray photoelectron spectroscopy of Ru-Zn catalysts for the partial hydrogenation of benzene. *Mol. Catal.* **2020**, *483*, 110710. [CrossRef]
5. Sun, H.J.; Chen, Z.H.; Li, C.G.; Chen, L.X.; Peng, Z.K.; Liu, Z.Y.; Liu, S.C. Selective hydrogenation of benzene to cyclohexene over Ru-Zn catalysts: Mechanism investigation on NaOH as a reaction additive. *Catalysts* **2018**, *8*, 104. [CrossRef]
6. Sun, H.J.; Chen, Z.H.; Li, C.G.; Chen, L.X.; Li, Y.; Peng, Z.K.; Liu, Z.Y.; Liu, S.C. Selective hydrogenation of benzene to cyclohexene over monometallic Ru catalysts: Investigation of ZnO and $ZnSO_4$ as reaction additives as well as particle size effect. *Catalysts* **2018**, *8*, 172. [CrossRef]

7. Sun, H.J.; Chen, Z.H.; Chen, L.X.; Li, H.J.; Peng, Z.K.; Liu, Z.Y.; Liu, S.C. Selective hydrogenation of benzene to cyclohexene over Ru-Zn catalysts: Investigations on the Effect of Zn content and ZrO_2 as the support and dispersant. *Catalysts* **2018**, *8*, 513. [CrossRef]
8. Liu, X.; Chen, Z.; Sun, H.; Chen, L.; Peng, Z.; Liu, Z. Investigation on Mn_3O_4 coated Ru nanoparticles for partial hydrogenation of benzene towards cyclohexene production using $ZnSO_4$, $MnSO_4$ and $FeSO_4$ as reaction additives. *Nanomaterials* **2020**, *10*, 809. [CrossRef] [PubMed]
9. Struijk, J.; Moene, R.; Kamp, T.V.D.; Scholten, J.J.F. Partial liquid phase hydrogenation of benzene to cyclohexene over ruthenium catalysts in the presence of an aqueous salt solution II. Influence of various salts on the performance of the catalyst. *Appl. Catal. A Gen.* **1992**, *89*, 77–102. [CrossRef]
10. Costa, G.P.; Gonçalves, A.H.A.; Viana, L.A.V.; Soares, J.C.S.; Passos, F.B.; Mends, F.M.T.; Gaspar, A.B. Role of $ZnNb_2O_6$ in ZnO-promoted amorphous-Nb_2O_5 supported Ru catalyst for the partial hydrogenation of benzene. *Mater. Today Chem.* **2021**, *19*, 100397. [CrossRef]
11. Spod, H.; Lucas, M.; Claus, P. Selective hydrogenation of benzene to cyclohexene over $2Ru/La_2O_3$-ZnO catalyst without additional modifiers. *ChemCatChem* **2016**, *8*, 1–9. [CrossRef]
12. Wang, J.Q.; Wang, Y.Z.; Xie, S.H.; Qiao, M.H.; Li, H.X.; Fan, K.N. Partial hydrogenation of benzene to cyclohexene on a Ru-Zn/m-ZrO_2 nanocomposite catalyst. *Appl. Catal. A Gen.* **2004**, *272*, 29–36. [CrossRef]
13. Zhang, P.; Wu, T.B.; Jiang, T.; Wang, W.T.; Liu, H.Z.; Fan, H.L.; Zhang, Z.F.; Han, B.X. Ru–Zn supported on hydroxyapatite as an effective catalyst for partial hydrogenation of benzene. *Green Chem.* **2013**, *15*, 152–159. [CrossRef]
14. Hu, S.C.; Chen, Y.W. Partial hydrogenation of benzene on Ru-Zn/SiO_2 catalysts. *Ind. Eng. Chem. Res.* **2001**, *40*, 6099–6104. [CrossRef]
15. Yuan, P.Q.; Wang, B.Q.; Ma, Y.M.; He, H.M.; Cheng, Z.M.; Yuan, W.K. Hydrogenation of cyclohexene over Ru-Zn/Ru(0001) surface alloy: A first principles density functional study. *J. Mol. Catal. A* **2009**, *301*, 140–145. [CrossRef]
16. Reddy, A.S.; Kim, J. An efficient g-C_3N_4-decorated CdS-nanoparticle-doped Fe_3O_4 hybrid catalyst for an enhanced H_2 evolution through photoelectrochemical water splitting. *Appl. Surf. Sci.* **2020**, *513*, 145836. [CrossRef]
17. Sun, H.J.; Wang, H.X.; Jiang, H.B.; Li, S.H.; Liu, S.C.; Liu, Z.Y.; Yuan, X.M.; Yang, K.J. Eeffect of $(Zn(OH)_2)_3(ZnSO_4)(H_2O)_5$ on the performance of Ru-Zn catalyst for benzene selective hydrogenation to cyclohexene. *Appl. Catal. A* **2013**, *450*, 160–168. [CrossRef]
18. Sun, H.J.; Jiang, H.B.; Dong, Y.Y.; Wang, H.X.; Pan, Y.J.; Liu, S.C.; Tang, M.S.; Liu, Z.Y. Effect of alcohols as additives on the performance of a nano-sized Ru-Zn(2.8%) catalyst for selective hydrogenation of benzene to cyclohexene. *Chem. Eng. J.* **2013**, *218*, 415–424. [CrossRef]
19. Sun, H.J.; Chen, L.X.; Huang, Z.X.; Liu, S.C.; Liu, Z.Y. Particle size effect of Ru-Zn catalysts on selective hydrogenation of benzene to cyclohexene. *Chem. J. Chin. Univ.* **2015**, *36*, 1969–1976.
20. Sun, H.J.; Li, Y.Y.; Li, S.H.; Zhang, Y.X.; Liu, S.C.; Liu, Z.Y.; Ren, B.Z. $ZnSO_4$ and La_2O_3 as Co-modifier of the monoclinic ru catalyst for selective hydrogenation of benzene to cyclohexene. *Acta Phys. Chim. Sin.* **2014**, *30*, 1332–1340.
21. Liu, J.L.; Zhu, L.J.; Pei, Y.; Zhuang, J.H.; Li, H.; Li, H.X.; Qiao, M.H.; Fan, K.N. Ce-promoted Ru/SBA-15 catalysts prepared by a "two solvent" impregnation method for selective hydrogenation of benzene to cyclohexene. *Appl. Catal. A Gen.* **2009**, *353*, 282–287. [CrossRef]
22. Sun, H.J.; Qin, H.A.; Huang, Z.X.; Su, M.F.; Li, Y.Y.; Liu, S.C.; Liu, Z.Y. Effect of reaction modifier $ZnSO_4$ and pretreatment on performance of Ru-Zn catalyst for selective hydrogenation of benzene to cyclohexene. *Chin. J. Inorg. Chem.* **2017**, *33*, 73–80.
23. Sun, H.J.; Pan, Y.J.; Jiang, H.B.; Li, S.H.; Zhang, Y.X.; Liu, S.C.; Liu, Z.Y. Effect of transition metals (Cr, Mn, Fe, Co, Ni, Cu and Zn) on the hydrogenation properties of benzene over Ru-based catalyst. *Appl. Catal. A Gen.* **2013**, *464–465*, 1–9. [CrossRef]
24. Yan, X.H.; Zhang, Q.; Zhu, M.Q.; Wang, Z.B. Selective hydrogenation of benzene to cyclohexene over Ru-Zn/ZrO_2 catalysts prepared by a two step impreganation method. *J. Mol. Catal. A Chem.* **2016**, *413*, 85–93. [CrossRef]
25. Ramos-Fernández, E.V.; Ferreira, A.F.P.; Sepúlveda-Escribano, A.; Kapteijn, F.; Rodríguez-Reinoso, F. Enhancing the catalytic performance of Pt/ZnO in the selective hydrogenation of cinnamaldehyde by Cr addition to the support. *J. Catal.* **2008**, *258*, 52–60. [CrossRef]
26. Ma, S.B.; Zhao, X.Y.; Li, Y.S.; Zhang, T.R.; Yuan, F.L.; Niu, X.Y.; Zhu, Y.J. Effect of W on the acidity and redox performance of the $Cu_{0.02}Fe_{0.2}W_aTiO_x$ (a = 0.01, 0.02, 0.03) catalysts for NH_3-SCR of NO. *Appl. Catal. B Environ.* **2019**, *248*, 226–238. [CrossRef]
27. Liu, L.J.; Xu, K.; Su, S.; He, L.M.; Qing, M.X.; Chi, H.Y.; Liu, T.; Hu, S.; Wang, Y.; Xiang, J. Efficient Sm modified Mn/TiO_2 catalysts for selective catalytic reduction of NO with NH_3 at low temperature. *Appl. Catal. A Gen.* **2020**, *592*, 117413. [CrossRef]
28. Azevedo, P.V.C.; Dias, M.V.; Gonçalves, A.H.A.; Borges, L.E.P.; Gaspar, A.B. Influence of cadmium on Ru/xCd/Al_2O_3 catalyst for benzene partial hydrogenation. *Mol. Catal.* **2021**, *499*, 111288. [CrossRef]